

Influence of substrate thickness on thermal impedance of microelectronic structures [☆]

B. Vermeersch ^{*}, G. De Mey

Ghent University, Department of Electronics and Systems (ELIS), Sint Pietersnieuwstraat 41, 9000 Gent, Belgium

Received 21 December 2005; received in revised form 17 May 2006

Available online 24 July 2006

Abstract

The thermal impedance $Z_{th}(j\omega)$ has been calculated numerically, using the boundary element method, for a silicon substrate with a uniform heat source on top. The key feature is that the dynamic thermal behaviour is calculated directly in the frequency domain. The calculations were performed for a wide range of values for the thickness of the substrate. By representing the thermal impedance in a Nyquist plot (i.e. $\text{Im}[Z_{th}(j\omega)]$ vs. $\text{Re}[Z_{th}(j\omega)]$ with ω as parameter), mainly two circular arcs are observed. For the lower frequency arc, the impedance values as well as the frequency scale are found to be largely influenced by the substrate thickness. The arc corresponding to high frequencies on the other hand remains unchanged under thickness variations.

Further analysis revealed an almost perfectly linear relationship between the thermal resistance $R_{th} = Z_{th}(j\omega = 0)$ and the substrate thickness, even when the heat source is not centred on the substrate. Both the slope and intersection value obtained from the curve fitting can be explained by a simple geometrical model including the fixed-angle heat spreading approximation, used since many years in the literature.

© 2006 Elsevier Ltd. All rights reserved.

1. Introduction

To characterise an electronic package thermally, the thermal resistance R_{th} is commonly used. By definition this is nothing else than the junction temperature T divided by the power P dissipated in the same junction, under the assumption that the ambient air is at a zero reference temperature. In other words, T denotes the relative temperature rise of the heat source to ambient.

The concept of thermal resistance can be easily extended to the frequency domain. The resulting complex quantity Z_{th} is called the thermal impedance and given by (in phasor notation):

$$Z_{th}(j\omega) = \frac{T(j\omega)}{P(j\omega)} \quad (1)$$

where ω is the angular frequency of the heat source. The thermal impedance Z_{th} can be seen as the thermal frequency response of the structure, which in fact captures the complete dynamic behaviour in an elegant and efficient way. Although pure AC thermal sources (having negative heat power dissipation each other half of the period) cannot exist in reality, the frequency response can be measured experimentally. Typically the transient temperature response to a power step or impulse is recorded. Fourier transformation of these data eventually leads to the complex thermal impedance [1,2].

The frequency dependency is visualised most commonly by means of a Nyquist curve, i.e. $\text{Im}[Z_{th}(j\omega)]$ vs. $\text{Re}[Z_{th}(j\omega)]$ with ω as a parameter. As it represents the frequency response, such a Nyquist plot can be seen as a thermal blueprint for the electronic structure [3]. Additionally, these thermal impedance curves have some interesting and powerful properties. Both experimental and theoretical

[☆] This paper was presented at the 1st European Advanced Technology Workshop (No formal technical paper required; no conference proceedings. A CD-ROM with PowerPoint presentations was distributed to the attendees only.) on Micropackaging and Thermal Management organised by IMAPS France, January 31–February 2, La Rochelle, France, 2006.

^{*} Corresponding author. Tel.: +32 9 264 89 52; fax: +32 9 264 89 61.

E-mail address: bjorn.vermeersch@elis.ugent.be (B. Vermeersch).

works have shown earlier that they are composed of a limited number of circular arcs [1,4–6], allowing a simple and compact description (centre coordinates and radii of the arcs) of the thermal impedance and thus the entire dynamic thermal behaviour. From the thermal impedance, one can also derive an equivalent thermal network, as demonstrated by Székely and his co-workers [7].

In this contribution we will consider a simple microelectronic structure consisting of a rectangular heat source mounted on a silicon substrate. The influence of the substrate thickness on the thermal impedance of the structure is investigated by means of numerical calculations. The obtained Nyquist plots are mainly composed of two circular arcs. The arc corresponding with the lower frequencies is largely influenced by the substrate thickness whereas the higher frequency part remains unchanged. The latter will be explained physically by considering a basic characteristic of thermal AC sources. Next, the thermal resistance is given a closer look to. A linear relation between R_{th} and the substrate thickness is observed, even when the heat source is not centred on the substrate. The curve fitting parameters extracted from the simulations correspond very well to those obtained by a simple geometrical model where a fixed angle heat spreading is assumed.

2. Numerical analysis

2.1. Boundary element method

A numerical approach offers the advantage that a lot of parameters, including structure dimensions and thermal parameters, can be varied. In addition, the method described hereafter has already proven its efficiency by reproducing experimentally measured thermal impedance curves [4].

We will calculate the thermal impedance of a structure directly in the frequency domain. The temperature distribution T (relative to ambient) in the material is obtained by solving the thermal conduction equation (in phasor notation):

$$k\nabla^2 T - j\omega C_v T = 0 \quad (2)$$

where k is the thermal conductivity (in W/m K) and C_v the specific heat per volume unit (in J/m³ K). For the numerical solution of (2), the boundary element method (BEM) will be used. Therefore, the fundamental solution of Eq. (2) is needed. This so-called Green's function is found to be [8]:

$$G(\vec{r}|\vec{r}') = \frac{1}{4\pi k|\vec{r} - \vec{r}'|} \exp\left(-\sqrt{\frac{j\omega C_v}{k}}|\vec{r} - \vec{r}'|\right) \quad (3)$$

in which \vec{r} and \vec{r}' denote the field point and source point respectively, and where $|\vec{r} - \vec{r}'|$ is the distance between the field and source point. After some manipulation, the following boundary integral can be obtained:

$$T(\vec{r}) = \int_S \int_S \left(G(\vec{r}|\vec{r}') \frac{\partial T(\vec{r})}{\partial n} - T(\vec{r}) \frac{\partial G(\vec{r}|\vec{r}')}{\partial n} \right) dS \quad (4)$$

This relates the temperature and its normal derivative in each point $\vec{r} \in S$ of the surface S of the material. Insertion of the boundary conditions and appropriate discretisation finally results in an algebraic set, from which the remaining unknowns (T or the normal derivative) are obtained.

For calculation of the thermal impedance the average source temperature is used, mainly because this is more representative than e.g. the maximum temperature. In practical experiments, thermal transient measurements are usually performed by recording the voltage drop over the junction. Based on a simple physical model, one can show this procedure approximately delivers a signal proportional to the average temperature of the device. Even then, the form of the Nyquist plots obtained for the maximum source temperature is essentially the same. Hence the choice for taking the average temperature does not change or limit the conclusions obtained in Section 3.

Repetition of the whole process for a wide range of frequency values finally leads to a Nyquist plot of the thermal impedance. Any further technical details about the BEM, including discretisation strategies and convergence issues, will be omitted here.

2.2. Boundary conditions

For the following, the bottom surface of the structure is assumed to be perfectly cooled: $T = 0$ (ideal heat sink), while the rest of the surface is supposed to be adiabatic (thermal isolation: $\frac{\partial T}{\partial n} = 0$). The only exception is the heat source, injecting a heat flux $q = k \frac{\partial T}{\partial n} = p$ into the material, where p is the uniform power density (in W/m²) of the source. Due to the small dimensions of microelectronic structures, the heat removal by either natural or forced convection can be reasonably neglected. This approximation is quite accurate in practice, especially for AC problems like we are studying here.

2.3. Benefits of the proposed technique

The key feature is the fact of the dynamic thermal behaviour being calculated directly in the frequency domain. This avoids sampling and aliasing issues which are likely to occur with more conventional techniques in the time domain followed by FFT.

In addition, the BEM which was proposed as numerical tool is expected to be both faster and more accurate compared with finite difference or finite element methods. Here only the outer surface of the material (instead of the entire volume) needs discretisation, explaining the speed gain. The increased accuracy is due to the fact that the BEM is based on an analytical solution (Eq. (3), i.e. the Green's function).

3. Results and discussion

3.1. Analyzed structure

We will investigate a structure that is roughly modelling a transistor or small integrated circuit on top of a semiconductor substrate. A uniform heat source ($50\ \mu\text{m} \times 50\ \mu\text{m}$) is centred on a square shaped substrate ($150\ \mu\text{m} \times 150\ \mu\text{m}$)—see Fig. 1. As an obvious example, silicon ($k = 160\ \text{W/m K}$, $C_v = 1.78 \times 10^6\ \text{J/m}^3\ \text{K}$) is chosen as substrate material. It has to be pointed out however that this particular choice will not play any role in further observations and conclusions. It can be proven that for a different isotropic material, the thermal impedance curve will show exactly the same shape. Just the impedance values and frequency along the curve need to be scaled [9]:

$$Z_2(j\omega_2) = \frac{k_1}{k_2} Z_1(j\omega_1) \quad \text{where} \quad \omega_2 = \frac{k_2}{k_1} \cdot \frac{C_{v1}}{C_{v2}} \cdot \omega_1 \quad (5)$$

More sophisticated (thermally engineered) materials are often anisotropic, e.g. $k_{\parallel} \neq k_z$. These cases can still be analyzed by considering an equivalent structure with isotropic conductivity k_{\parallel} and thickness scaled with a factor $\sqrt{\frac{k_{\parallel}}{k_z}}$.

The thickness of the substrate will be varied over a wide range ($H = 50\text{--}250\ \mu\text{m}$). For each chosen value the thermal impedance is calculated numerically, using the aforementioned procedure.

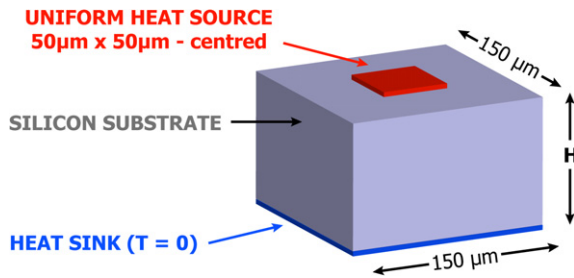


Fig. 1. Analyzed structure: heat source mounted on silicon substrate with thickness H .

3.2. Thermal impedance for various substrate thicknesses

Some calculated thermal impedance plots are presented in Fig. 2. In all cases, the Nyquist plot is composed of two circular arcs. For particular points, namely those where $\text{Im}[Z_{\text{th}}]$ reaches a minimum, the corresponding frequency—the so called central frequency of the arc—is marked. Putting all the curves on the same graph provides the advantage of seeing very easily that all the higher frequency arcs coincide. This holds for the impedance values as well as for the frequency scale. In other words, above a certain frequency the thermal impedance is not influenced by the substrate thickness. This topic will be discussed further in the next section.

As one can observe in Fig. 2, the lower frequency arc on the other hand is largely affected by the substrate thickness. First of all, and not surprisingly, the impedance values grow as H increases. Making the substrate thicker deteriorates indeed the heat removal capabilities of the structure, resulting in higher thermal impedances. In addition, the size is not the only property of the arc being influenced. Both the extent to which the circle is traversed and the involved frequencies are subject to change under thickness variations. Clearly, the central frequency of the arc tends to drop as the thickness increases.

3.3. Insensitivity of higher frequency arc

As mentioned before, the higher frequency part of the thermal impedance of the structure is not influenced by the substrate thickness. This can be explained by taking into account the oscillating nature of the heat source. Roughly speaking, the temperature field generated by a thermal AC source is exponentially decaying in space. Therefore only a limited amount of material will be considerably heated by the source, and the size of the heated region is closely related to the AC temperature decay length. For the latter, the following rule of thumb applies:

$$\text{decay length} \propto \frac{1}{\sqrt{\omega}} \quad (6)$$

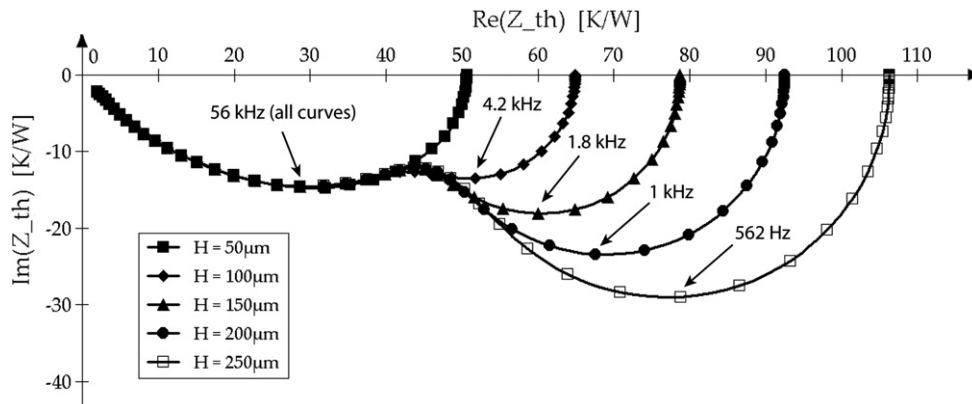


Fig. 2. Nyquist plots of thermal impedance for various thickness values.

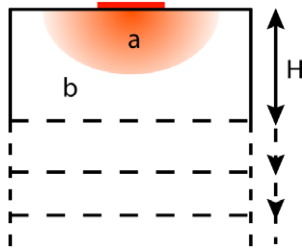


Fig. 3. High frequency behaviour: (a) heated region, (b) almost at ambient temperature.

This behaviour can easily be understood by looking at the Green's function given by Eq. (3). In simple words, the heated region gets smaller and smaller as the frequency of the heat source is rising. For the analyzed structure, only the upper part of the silicon (regions closest to the heat source) is substantially heated once a certain frequency has been reached (Fig. 3). At that point, the other parts of the substrate are almost at ambient temperature. As a consequence, the amount of material underneath the heated region does not have any influence on the thermal AC behaviour of the substrate. In other words, it does not matter how thick the substrate is, which finally explains why the influence of the substrate thickness on the thermal impedance disappears at sufficiently high frequencies.

3.4. Relation between thermal resistance and substrate thickness

Let us now take a closer look at the thermal resistance of the substrate. In the context of this paper, the thermal resistance corresponds with the “starting point” of the Nyquist plots and is nothing else than the thermal impedance at DC conditions ($j\omega = 0$). Fig. 4 shows the values obtained from the numerical calculations as function of the substrate thickness H .

This thermal resistance versus thickness graph is looking very similar to those that have been reported before [10]. Apart from the “transition phenomenon” for small thickness values, a linear curve fitting is nearly perfect. This corresponds with a relation of the form:

$$R_{th} = R_0 + \alpha \cdot H \quad (7)$$

The curve fitting values for the slope α and intersection R_0 are indicated in Fig. 4. It should be noted that R_0 is NOT equal to zero. For very thin substrates however the relation (7) starts to fail. When $H \rightarrow 0$, bringing heat source and heat sink closer and closer to each other, the source gets eventually perfectly cooled for $H = 0$ and the thermal resistance disappears.

3.5. Comparison to geometrical heat spreading model

For quick estimations of the thermal resistance, a fixed heat spreading angle approximation is often used [10–15]. The assumption is that the heat dissipated by the source spreads uniformly into the substrate under a fixed angle Φ , with the isothermal surfaces being horizontal planes. Once the spreading heat “touches” the side walls of the substrate, at a depth L in the substrate, the previous assumptions lead to a linear 1-D temperature drop across the remaining thickness $H - L$ of the material. This model suggests two contributions to the thermal resistance (Fig. 5):

$$R_{th} = R_{geo} + R_{bulk} \quad (8)$$

R_{geo} —sometimes called geometrical contact resistance—is the thermal resistance of the pyramid corresponding to the fixed angle heat spreading. R_{bulk} is the resistance of the remaining material block and is given by Pouillet's law:

$$R_{bulk} = \frac{H - L}{k \cdot A} \quad (9)$$

where A is the area of the cross-section of the substrate. Introduction of this result in Eq. (8) yields:

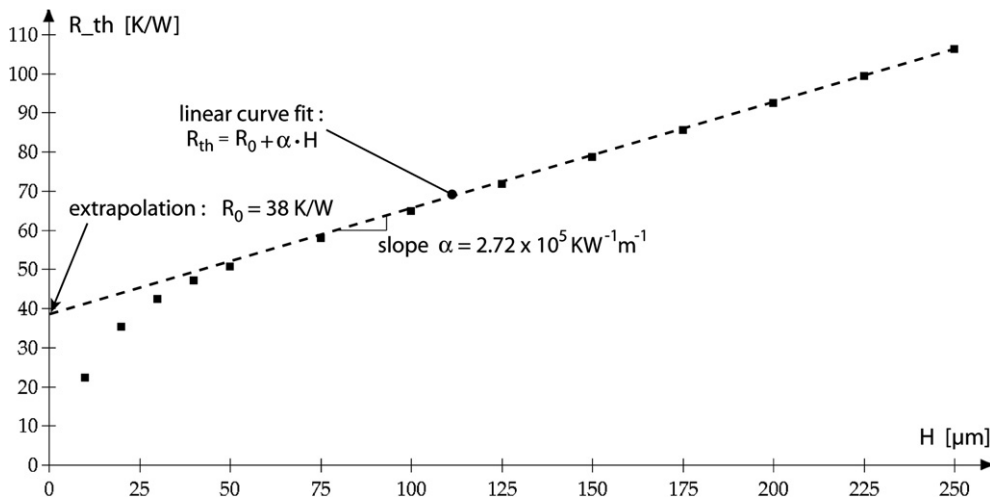


Fig. 4. Thermal resistance versus substrate thickness.

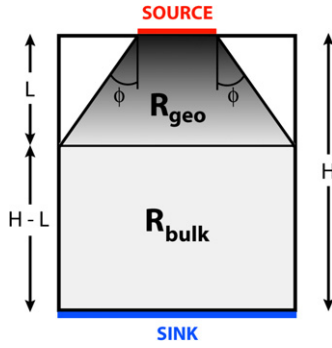


Fig. 5. Geometrical model for thermal resistance.

$$R_{th} = \underbrace{\left(R_{geo} - \frac{L}{kA} \right)}_{R_0} + \underbrace{\frac{1}{kA}}_{\alpha} \cdot H \quad (10)$$

which is exactly the same form as observed for the simulation results—see Eq. (7). Both R_0 and α can be easily identified in terms of the geometrical parameters.

For the calculation of R_{geo} , we suppose a square heat source (side w) being centred on a substrate with square shaped cross-section (side W). It is clear that the analyzed structure from Fig. 1 meets these requirements. A horizontal slice with infinitely small thickness dz at depth z of the pyramid is then contributing (see Fig. 6):

$$dR_{geo} = \frac{dz}{k(w + 2z \cdot \tan \Phi)^2} \quad (11)$$

The total resistance R_{geo} of the pyramid is nothing else than the resistance of all the slices put in series which leads to:

$$R_{geo} = \int_{z=0}^{z=L} dR_{geo} = \frac{1 - w/W}{2w \cdot k \cdot \tan \Phi} \quad (12)$$

in which we used the fact that $L = \frac{W-w}{2 \tan \Phi}$. For simplicity reasons, a heat spreading angle of 45° is the most common choice. However, it has been shown that $\Phi = 32.5^\circ$ produces the best overall results for a wide variety of geometries [11,12]. Using this value, together with $w = 50 \mu\text{m}$, $W = 150 \mu\text{m}$ and $k = 160 \text{ W/m K}$, leads to $L = 78 \mu\text{m}$ and $R_{geo} = 65.4 \text{ K/W}$. Based on these results, the geometrical model predictions for the slope and intersection values can be found using Eq. (10). As one can see in Table 1, the

Table 1

Influence of substrate thickness on thermal resistance: simulation results versus geometrical heat spreading model

	$R_{th} = R_0 + \alpha \cdot H$	
	Curve fitting for simulation results	Heat spreading model
R_0	38 K/W	43.7 K/W
α	$2.72 \times 10^5 \text{ K/W m}$	$2.78 \times 10^5 \text{ K/W m}$

resulting α and R_0 are in close agreement with the curve fitting parameters from Fig. 4. It proves that the proposed heat spreading model with $\Phi = 32.5^\circ$ is quite accurate for the investigated structure. Using a heat spreading angle of 45° yields $R_0 = 13.9 \text{ K/W}$, clearly being a very poor estimation.

Instead of using the literature values we have mentioned, the spreading angle Φ (and hence L) can also be estimated directly from the simulation results. Based on Eqs. (10) and (12) one obtains:

$$\tan(\Phi) = \frac{(W - w)(W/w - 1)}{2kW^2R_0} \quad (13)$$

The extrapolation value R_0 was determined for some materials commonly found in electronic packages. The resulting heat spreading angles are listed in Table 2. For the wide range of $k = 4\text{--}380 \text{ W/m K}$, the spreading angle hardly changes: $\Phi \approx 36.5^\circ$ ($L = 68 \mu\text{m}$). Clearly, this is an illustration of Eq. (5): the qualitative results are not depending on the particular thermal properties of the substrate material.

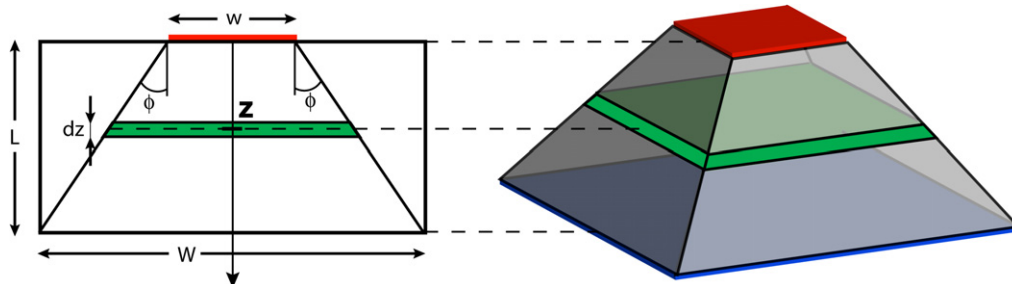
3.6. Non-symmetric source configurations

It is interesting to point out that many of the conclusions made earlier, still hold for cases where the heat source

Table 2

Estimated heat spreading angle for various materials

Material	k [W/m K]	C_p [$10^6 \text{ J/m}^3 \text{ K}$]	Φ [deg]
LTCC	4	2.38	36.5
Al_2O_3	22	2.98	36.8
GaAs	50	1.86	36.5
Si	160	1.78	36.2
AlSiC	200	2.23	36.5
Cu	380	3.47	36.5

Fig. 6. Calculation of heat spreading resistance R_{geo} .

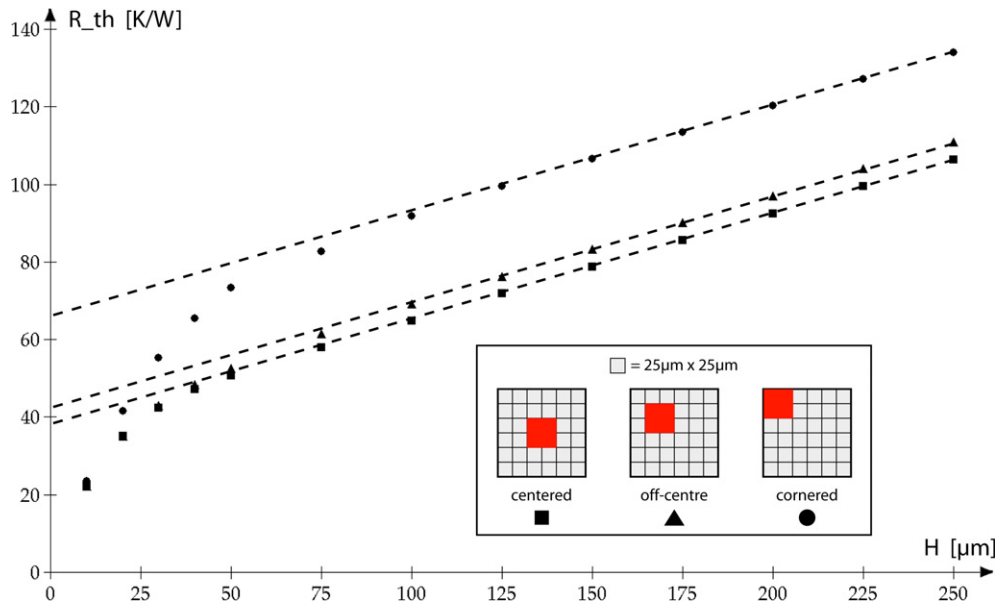


Fig. 7. Thermal resistance versus substrate thickness for various source configurations.

is not centred on the substrate. Fig. 7 compares the calculated thermal resistance as a function of the substrate thickness for three different configurations (centred, off-centre and cornered source). For the latter two cases, a linear curve fitting approximation is still nearly perfect. The thermal resistance increases as the source is moving further away from the centre of the substrate. This can be easily explained: sources closer to the corner are getting closer to the adiabatic side walls of the substrate, where the heat will tend to accumulate. The heat removal is less efficient compared to the centred source and therefore we observe a rise of the thermal resistance.

More importantly, all curve fittings on Fig. 7 show the same slope. This indicates that the geometrical model, and Eq. (10) in particular, remains valid for the non-symmetric configurations. Interpretation and calculation of R_{geo} is however much more complicated as the heat spreading pyramid will touch some side walls earlier than others.

The conclusions concerning the complex thermal impedance Z_{th} also still hold. Some Nyquist plots for the off-centre source are shown in Fig. 8. Again two circular arcs are observed. For each arc, the behaviour with respect to thickness variations is the same as observed earlier in Sections 3.2 and 3.3 for the centred source. The difference between the two configurations (off-centre vs. centre source) reveals itself in the Nyquist plot by the slightly different shape of the higher frequency arc, and a shift in some central frequencies.

4. Summary

Through numerical calculations, we have investigated the influence of substrate thickness on the complex thermal impedance of a simple microelectronic structure. Silicon was used as the substrate material, but it was pointed out that any other isotropic materials would give rise to the

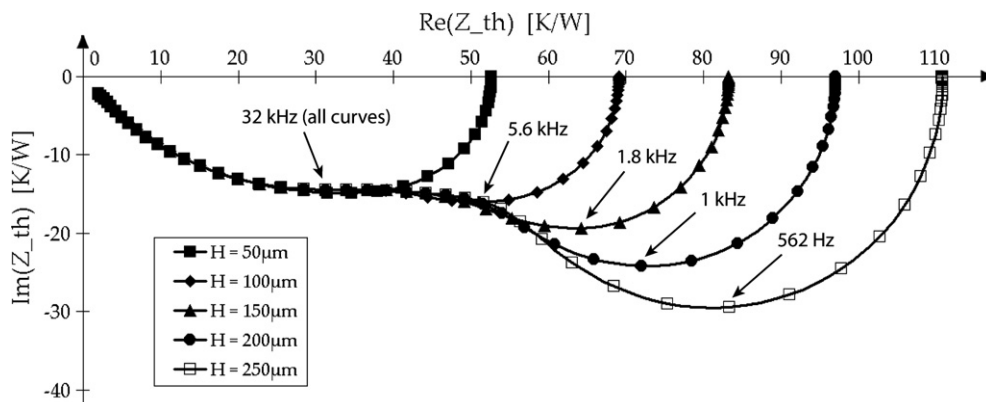


Fig. 8. Nyquist plots of thermal impedance for various thickness values (off-centre source—see Fig. 7).

same conclusions. For a wide range of thickness values, the Nyquist plot of the thermal impedance is composed of two circular arcs. The higher frequency arc remains the same under thickness variations, which was explained by considering the frequency dependent decay length of the AC temperature distribution. For the arc corresponding to the lower frequencies, an expansion of the arc as well as a shift in the frequency scale was noticed as the substrate gets thicker. When it comes to the thermal resistance as function of the substrate thickness, the calculation results could be fitted almost perfectly with a straight line. Both this linear behaviour in general and the curve fitting parameters corresponded very well to the thermal resistance obtained by a geometrical model for the heat spreading through the substrate. Finally, it was demonstrated that the phenomena we have observed are not provoked by the symmetry of the structure: many of the aforementioned conclusions remain valid for a structure where the heat source is not centred on top of the substrate.

Acknowledgement

This research was supported by the Research Foundation—Flanders (FWO—Vlaanderen).

References

- [1] Kawka P. Thermal impedance measurements and dynamic modelling of electronic packages. PhD thesis, University of Ghent, Belgium, 2005.
- [2] Christiaens F, Vandeveld B, Beyne E, et al. A generic methodology for deriving compact dynamic thermal models, applied to the PSGA package. *IEEE Trans Compon Pack Manuf Technol Part A* 1998; 21(4):565–76.
- [3] De Mey G, Vermeersch B, Kawka P. Thermal characterization of electronic packages using the Nyquist plot of the thermal impedance. In: 1st European advanced technology workshop on micropackaging and thermal management, La Rochelle, France, 2006. Technical presentations CD-ROM.
- [4] De Mey G, Vermeersch B, Kawka P. Thermal impedance simulations of electronic packages. In: Napieralski A, editor. Proceedings of the 12th international conference on mixed design and integrated circuits and systems (MIXDES 2005), Krakow, Poland, 2005. p. 267–9.
- [5] Vermeersch B, De Mey G. Thermal impedance plots of micro-scaled devices. *Microelectron Reliab* 2006;46(1):174–7.
- [6] Székely V. Identification of RC networks by deconvolution: chances and limits. *IEEE Trans Circuits Syst I—Regul Pap* 1998;45(3): 244–58.
- [7] Székely V, Van Bien T. Fine structure of heat flow path in semiconductor devices: a measurement and identification method. *Solid-State Electron* 1988;31(9):1363–8.
- [8] De Mey G. Various applications of the boundary element method. Oradea: University of Oradea (Romania); 2002. p. 61–2.
- [9] Vermeersch B. Thermische diffusie in sinusregime (in Dutch). Master thesis, University of Ghent, Belgium, 2005.
- [10] Guenin BM. The 45° heat spreading angle—an urban legend? *Electron Cooling* 2003;9(4):10–2.
- [11] David RF. Computerized thermal analysis of hybrid circuits. *IEEE Trans Parts, Hybr Packag* 1977;13(3):283–90.
- [12] Zimmer CR. Computer simulation of hybrid integrated circuits including combined electrical and thermal effects. In: Proc of third European hybrid microelectronics conference, Avignon, France, 1981. p. 44–50.
- [13] Dean DJ. Thermal design of electronic circuit boards and packages. Ayr: Electrochemical Publications; 1985. p. 75–90.
- [14] Dobbelaere W, Matthys L, De Baetselier E, Goedertier W, De Mey G. Heat spreading angles in multilayer structures. In: Proc 3rd advanced training course mixed design of integrated circuits and systems (MIXDES96), Lodz, Poland, 1996. p. 238–43.
- [15] Masana FN. A closed form solution of junction to substrate thermal resistance in semiconductor chips. *IEEE Trans Compon Packag Manuf Technol A* 1996;19(4):539–45.